Phase compatibility and thermoelectric properties of compounds in the Sr–Ca–Co–O system

W. Wong-Ng,[a] G. Liu, J. Martin, E. L. Thomas, N. Lowhorn, and J. A. Kaduk[b]
Ceramics Division, NIST, Gaithersburg, Maryland 20899, USA

(Received 21 September 2009; accepted 24 November 2009; published online 3 February 2010)

Two low-dimensional cobaltite series in the Sr–Ca–Co–O system have been investigated for their solid solution limit, structure, and compatibility phase relationships (850 °C in air). Thermoelectric properties have been measured for selected members of these solid solutions. In $(Ca,Sr)_3Co_4O_9$, which has a misfit layered structure, Sr was found to substitute in the Ca site to a limit of $(Ca_{0.8}Sr_{0.2})_3Co_4O_9$. Compounds in the homologous series, $A_{n+2}Co_nCo'O_{3n+3}$ [where A=Sr, Ca, (Ca,Sr), or (Sr,Ca)], consist of one-dimensional parallel $Co_2O_6^{6-}$ chains that are built from successive alternating face-sharing CoO_6 trigonal prisms and "n" units of CoO_6 octahedra along the hexagonal *c*-axis. In the $Ca_{n+2}Co_nCo'O_{3n+3}$ series, only the n=1 phase ($Ca_3Co_2O_6$) could be prepared under the present synthesis conditions. Sr substitutes in the Ca site of $Ca_3Co_2O_6$ to a limit of $(Ca_{0.9}Sr_{0.1})_3Co_2O_6$. In the $Sr_{n+2}Co_nCo'O_{3n+3}$ series, Ca substitutes in the Sr site of the n=2, 3, and 4 members to a limit of $(Sr_{0.7}Ca_{0.3})_4Co_3O_9$, $(Sr_{0.67}Ca_{0.33})_5Co_4O_{12}$, and $(Sr_{0.725}Ca_{0.275})_6Co_5O_{15}$, respectively. While the members of the $Ca_{n+2}Co_nCo'O_{3n+3}$ and $Sr_{n+2}Co_nCo'O_{3n+3}$ series have reasonably high Seebeck coefficients and relatively low thermal conductivity, the electrical conductivity needs to be increased in order to achieve high *ZT* values. [doi:10.1063/1.3276158]

I. INTRODUCTION

Over the past decade, the increasing global interest in research and development on thermoelectric (TE) materials was partly due to the soaring demand for energy and partly due to the need to create a sustainable energy future. The efficiency and performance of TE energy conversion or cooling is related to the dimensionless figure of merit (*ZT*) of the TE materials, given by $ZT=S^2\sigma T/\kappa$, where *T* is the absolute temperature, *S* is the Seebeck coefficient or TE power, σ is the electrical conductivity, and *k* is the thermal conductivity.[1] *ZT* is directly related to the coefficient of performance of a TE material. For almost half a decade, only a small number of materials have been found to have practical industrial applications and they all have *ZT* values around or below 1.0. Optimization of the *ZT* values is not a straightforward process because *S*, σ, and κ are interrelated. Recent reports that relatively high *ZT* values are possible in both thin film and bulk forms[2–7] have revitalized interest in TE material development.

The stability of TE oxides at high temperature has made them highly relevant to waste heat conversion applications. For example, the low-dimensional cobaltites that include $NaCoO_x$,[8] $Ca_2Co_3O_6$,[9,10] and $Ca_3Co_4O_9$ (Refs. 11–14) exhibit the coexistence of large Seebeck coefficient and relatively low thermal conductivity. Consequently in recent years, considerable research has been conducted on TE oxides.

Phase equilibrium diagrams provide road maps for processing and facilitate an understanding of materials properties. Because of the promising properties of calcium-containing cobaltite, strontium-doped calcium cobaltites may also offer desirable properties. This paper discusses the phase compatibility relationships, crystal chemistry, crystallography, and TE property measurements of selected series of compounds in the Ca–Sr–Co–O system, including $(Ca,Sr)_3Co_4O_9$ and the homologous series $A_{n+2}Co_nCo'O_{3n+3}$, where A=Sr, Ca, (Ca,Sr), and (Sr, Ca).

II. EXPERIMENTAL

A. Sample preparation

Using the high temperature solid-state methods, 54 samples were prepared from stoichiometric amounts of $CaCO_3$, Co_3O_4, and $SrCO_3$ (Table I). These samples were mixed, pelletized, and annealed at 750 °C for 1 day, and subsequently annealed at 850 °C with intermediate grindings and pelletizations for another 7 days. The annealing process was repeated until no further changes were detected in the powder x-ray diffraction patterns.

Powder x-ray diffraction was used to investigate phase purity and establish phase relationships. These experiments were carried out using a Phillips x-ray powder diffractometer with Cu Kα radiation and equipped with a series of soller slits and a scintillation counter. The 2θ scanning range was from 10° to 80°, and the step interval was 0.03°. The ICDD PDF reference diffraction patterns of the Ca–Sr–Co–O systems[15] were used for performing phase identification.

The x-ray Rietveld refinement technique (GSAS suite)[16] was used to confirm the single phase nature of some of the phases as well as the structure of phases of interest. A Bruker D8 advanced diffractometer[17] that is equipped with a VANTEC-1 position-sensitive detector was used to measure the powder patterns (Cu Kα radiation, 40 kV, 40 mA) from 5° to 150° 2θ in 0.0073° steps, counting for 0.5 s/step. The

[a]Electronic mail: winnie.wong-ng@nist.gov.
[b]INEOS Technologies, Naperville, IL 60566.

TABLE I. Samples prepared for the phase equilibrium study of the Sr–Ca–Co–O system at 850 °C in air.

No.	Sr	Ca	Co
1	0	0.6	0.4
2	0.6	0	0.4
3	0.285 7	0.285 7	0.4286
4	0	0.428 6	0.5714
5	0.5	0	0.5
6	0.545 45	0	0.4546
7	0.555 6	0	0.4444
8	0.12	0.48	0.4
9	0.24	0.36	0.4
10	0.36	0.24	0.4
11	0.48	0.12	0.4
12	0.171 42	0.4	0.4286
13	0.399 98	0.171 4	0.4286
14	0.571 4	0	0.4286
15	0.444 4	0.111 2	0.4444
16	0.370 4	0.185 2	0.4444
17	0.333 3	0.222 2	0.4444
18	0.45	0.05	0.5
19	0.4	0.1	0.5
20	0	0.5	0.5
21	0.45	0	0.55
22	0.085 71	0.342 9	0.571 4
23	0.142 86	0.285 7	0.5714
24	0.214 29	0.214 3	0.5714
25	0.3	0	0.7
26	0.15	0.15	0.7
27	0	0.2	0.8
28	0	0.05	0.95
29	0.05	0	0.95
30	0	0	1
31	0	0.1	0.9
32	0.3	0.3	0.4
33	0.06	0.54	0.4
34	0.03	0.57	0.4
35	0.1	0.4	0.5
36	0.042 87	0.385 7	0.5714
37	0.128 57	0.3	0.5714
38	0.305 6	0.25	0.4444
39	0.320 45	0.225	0.4546
40	0.395 45	0.15	0.4546
41	0.475	0.070 5	0.4546
42	0.523 81	0	0.4762
43	0.4	0.123 8	0.4762
44	0.35	0.173 8	0.4762
45	0.4	0.028 6	0.5714
46	0.3	0.271 4	0.4286
47	0.1	0.5	0.4
48	0.471 4	0.1	0.4286
49	0.45	0.073 8	0.4762
50	0.475	0.025	0.5
51	0.4	0.5	0.1
52	0.075	0.725	0.2
53	0.55	0.15	0.3
54	0.25	0.4	0.35

specimens were mounted as acetone slurries on zero-background cells and were rotated rapidly during data collection. The background was fitted by a six-term shifted Chebyshev function.

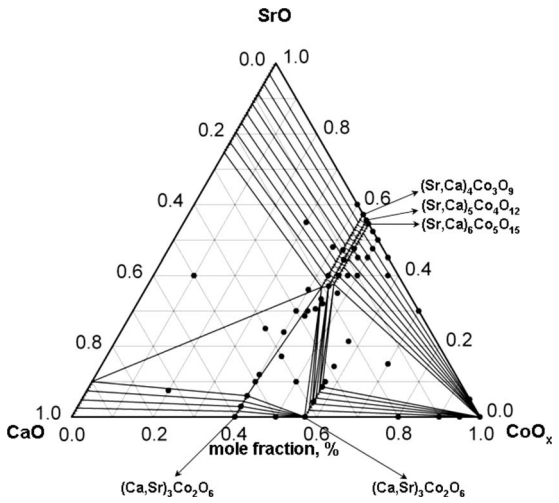

FIG. 1. Phase diagram of the SrO–CaO–CoO$_x$ system at 850 °C, showing the limits of various solid solutions and the tie-line relationships of various phases.

B. TE property measurements

The bulk samples were pressed into disks and sintered at 850 °C. The pressed polycrystalline specimens were then cut into $\approx 1.5 \times 2 \times 8$ mm^3 parallelepipeds for transport property measurements. A high throughput power factor ($S^2\sigma$) screening tool[18,19] was used to screen the Seebeck coefficient and resistivity of the flat surface of the bulk samples to ensure a reasonable power factor value at room temperature before conducting a more time-consuming measurement. ac resistivity, two-probe Seebeck coefficient and thermal conductivity were measured using continuous gradient techniques (TTO option) in a Quantum Design physical property measurement system,[17,20] from 390 to 2 K. The cooling rate was 0.5 K/min with a thermal gradient within 3% of the base temperature, and the ac was adjusted between 0.1 and 75 mA at 10–300 Hz. Copper bars (cross section: 0.24×0.64 mm^2) were silver epoxy bonded to nickel plated specimen surfaces for Ohmic contacts.

III. RESULTS AND DISCUSSION

Figure 1 gives the phase diagram of the Sr–Ca–Co–O system that was determined at 850 °C in air. The phase relationships between solid solutions and other phases are expressed as tie-line bundles. The crystal chemistry, crystallography, and TE properties of various phases in the binary as well as the ternary oxide systems are discussed below.

A. SrO–CaO

No intermediate phases form in this system other than the (Sr,Ca)O and (Ca,Sr)O solid solutions. According to Roth *et al.*,[21] there is a miscibility gap between the SrO and CaO end members below approximately 950 °C. At 875 °C, the extent of the solid solutions have been determined to be $(Sr_{0.75}Ca_{0.25})O$ and $(Ca_{0.9}Sr_{0.1})O$.

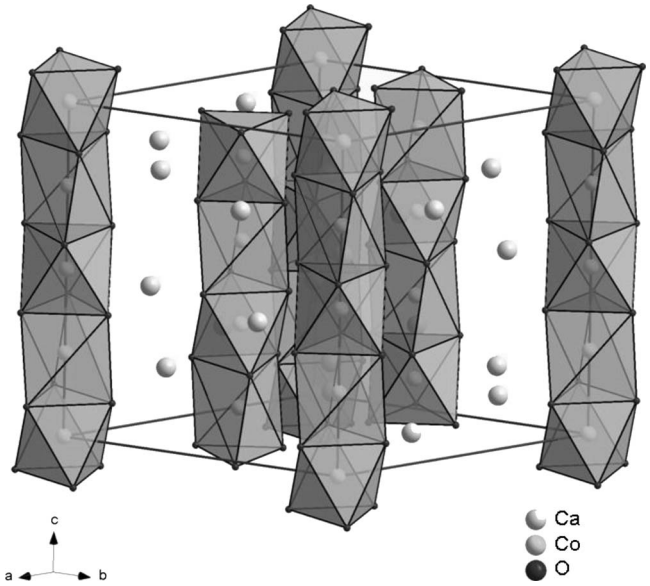

FIG. 2. Crystal structure of $Ca_3Co_2O_6$ (n=1 member in the homologous series, $Ca_{n+2}Co_nCoO_{3n+3}$), showing the feature of linear chains of successive alternations of CoO_6 octahedron with CoO_6 prism.

B. CaO–CoO_x

Two binary phases were determined in this system, namely, $Ca_3Co_2O_6$ and $Ca_3Co_4O_9$. The $Ca_3Co_4O_9$ phase has been extensively studied.[11–14,22] $Ca_3Co_4O_9$ is a misfit layered oxide that has two monoclinic subsystems with identical *a*, *c*, and β but different *b*.[12] The first subsystem consists of triple rock-salt layers of Ca_2CoO_3 in the *ab* plane, while the second subsystem consists of a single CoO_2 layer, which has the CdI_2-type structure. This phase exhibits strong anisotropic TE properties in the *ab* plane. It is thought that the increased scattering of phonons at the interface of misfit layers leads to the lowering of the lattice thermal conductivity. The chemical formula can be written as $[Ca_2CoO_3]RS\ [CoO_2]_{1.61}$, where RS is the rock salt and 1.61 expresses the incommensurable character for the *b* parameter of the rock salt and the CdI_2-type structure.

$Co_3Co_2O_6$ [$R\bar{3}c$, $a=9.0793(7)$ Å, and $c=10.381(1)$ Å;[23] Fig. 2] is the n=1 member of the homologous series with the general formula of $A_{n+2}B_nB'O_{3n+3}$, where A is an alkali-earth element such as Ca, Sr, and Ba. B describes the cobalt ion inside the octahedral cage, and B′ is the cobalt ion inside a trigonal prism. $Ca_{n+2}Co_nCoO_{3n+3}$ consists of one-dimensional linear parallel $Co_2O_6^{6-}$ chains, built by successive alternating face-sharing CoO_6 trigonal prisms and CoO_6 octahedra along the hexagonal *c*-axis.[24] This face-sharing feature is in contrast with $Ca_3Co_4O_9$ (Ref. 12) and $NaCo_2O_4$ (Ref. 8) which consists of edge-sharing CoO_6 octahedra. The linear $Co_2O_6^{6-}$ chains of $Ca_3Co_2O_6$ consist of one CoO_6 octahedron alternating with one CoO_6 trigonal prism. Each $Co_2O_6^{6-}$ chain is surrounded by six other chains which form a hexagonal arrangement. These $Co_2O_6^{6-}$ chains are separated by octacoordinated Ca^{2+} ions (Fig. 3). The compounds $A_{n+2}Co_nCo'O_{3n+3}$ can also be considered as ordered intergrowth between the n=∞ ($ACoO_3$) and n=1 ($A_3Co_2O_6$) end members.[25,26] We found that when A=Ca, only the n=1 member, namely, $Ca_3Co_2O_6$, can be made.

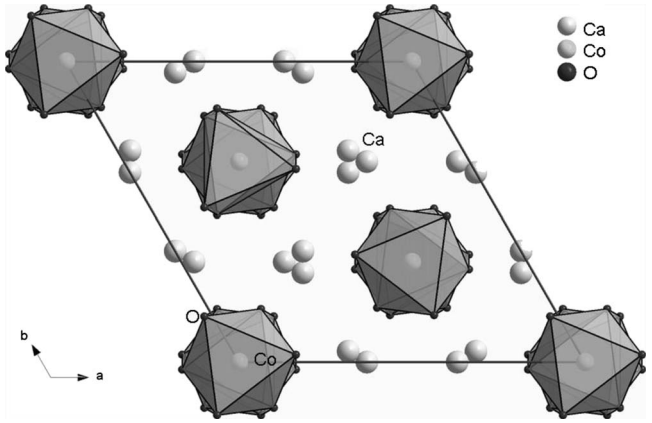

FIG. 3. Crystal structure of $Ca_3Co_2O_6$, showing each $Co_2O_6^{6-}$ chain being surrounded by six other chains. These $Co_2O_6^{6-}$ chains are separated by octacoordinated Ca^{2+} ions

C. SrO–CoO_x

The only phase found in the SrO–CoO_x system is the homologous series $Sr_{n+2}Co_nCo'O_{3n+3}$. The stable $Sr_{n+2}Co_nCo'O_{3n+3}$ compounds for the relatively larger Sr (as compared to Ca in $Ca_{n+2}Co_nCoO_{3n+3}$) are those with $2 \leq n < 5$. The n=1 member ($Sr_3Co_2O_6$) cannot be prepared. The x-ray diffraction pattern of the composition $Sr_3Co_2O_6$ gives a mixture of $Sr_4Co_3O_9$ and SrO. Figure 4 gives x-ray diffraction patterns for the n=2, 3, and 4 members of the $Sr_{n+2}Co_nCo'O_{3n+3}$ series. The n=2 member, $Sr_4Co_3O_{10}$, has been reported to be isostructural with $Sr_4Ni_3O_{10}$[27] (Fig. 5). From x-ray diffraction, the space group and unit cell parameters of $Sr_4Co_3O_{10}$ are determined to be *P*321, $a=9.5074$ Å, and $c=7.9175$ Å. In the $Co_3O_{10}^{8-}$ chains, there are two units of CoO_6 octahedra alternating with a CoO_6 prism.[26] The structures for the n=3 and n=4 members, namely, $Sr_5Co_4O_{11}$ (*P*3*c*1, $a=9.4$ Å, $c=20.2$ Å,[26] Fig. 6) and $Sr_6Co_5O_{15}$ [*R*32, $a=9.5035(2)$ Å, $c=12.3966(4)$ Å,[28] Fig. 7] feature three and four octahedra interleaving with one trigonal prism along the *c*-axis, respectively. We were not able to make the n≥5 phases; however, the $(Ba_{0.5}Sr_{0.5})_7Co_6O_{18}$, $Ba_8Co_7O_{21}$, and $Ba_9Co_8O_{24}$ phases were reported by Boulahya *et al.*[25,26]

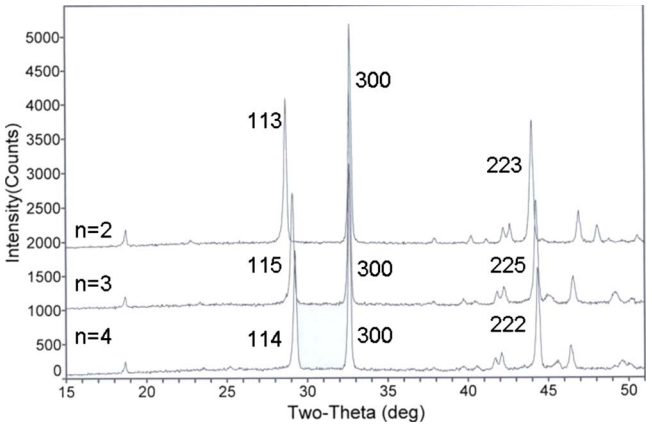

FIG. 4. (Color online) X-ray diffraction patterns for n=2, 3, and 4 members of $Sr_{n+2}Co_nCoO_{3n+3}$. Selected *hkl* indices are given.

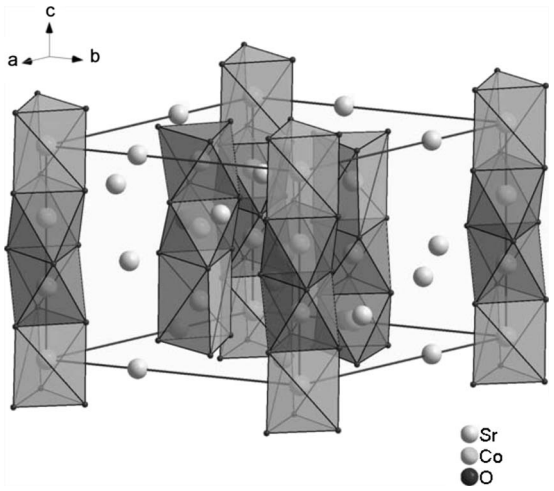

FIG. 5. Crystal structure of $Sr_4Co_3O_9$ [isostructural to $Sr_4Ni_3O_9$[26], n=2 member in the homologous series, $Sr_{n+2}Co_nCoO_{3n+3}$], showing the feature of linear chains of successive alternations of two units of CoO_6 octahedra with a CoO_6 prism.

Although the $BaCoO_3$ structure with linear chains exists (Fig. 8),[25] the n=∞ hexagonal Sr analog does not form under the current conditions. X-ray Rietveld refinement of a powder sample of composition of $SrCoO_3$ gave a mixture of Co_3O_4 and the n=4 member or $Sr_6Co_5O_{15}$. There appears to be a general trend that the ionic radius[29] of the alkaline-earth metals of A increases with the increasing number of n resulting in stable $Sr_{n+2}Co_nCo'O_{3n+3}$ phases. For example, the n =1 compound has been reported with A=Ca; n=2, 3, and 4 with A=Sr, and n=5 and 6 with A=Ba.[26] According to Boulahya *et al.*,[25,26] these compounds can be considered as making up of A_3O_9 layers as well as liner parallel chains of cobalt oxides. In order to stabilize the n≥5 members of the $A_{n+2}Co_nCo'O_{3n+3}$ series, it is necessary to increase the distance between the AO_3 layers by increasing the size of the cations in A positions.

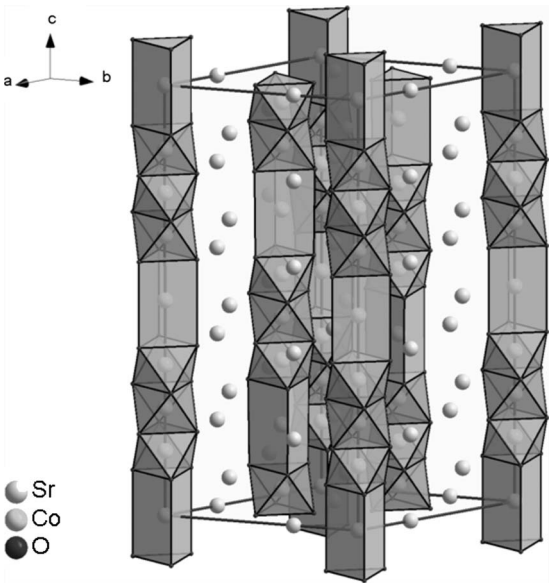

FIG. 6. Crystal structure of $Sr_5Co_4O_{11}$ (n=3 member in the homologous series, $Sr_{n+2}Co_nCoO_{3n+3}$), showing the feature of linear chains of successive alternations of three units of CoO_6 octahedra with an CoO_6 prism.

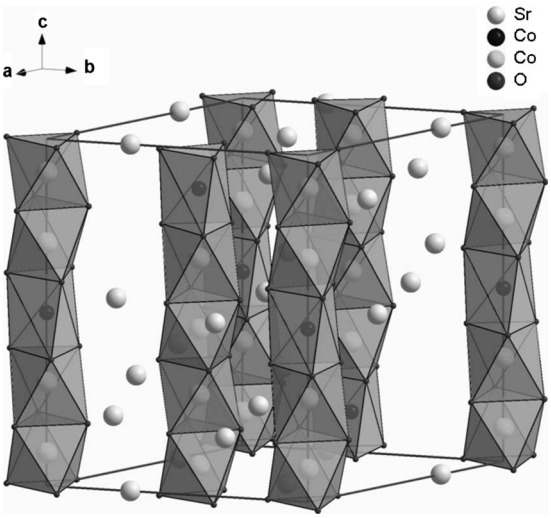

FIG. 7. Crystal structure of $Sr_6Co_5O_{13}$ (n=4 member in the homologous series, $Sr_{n+2}Co_nCoO_{3n+3}$), showing the feature of linear chains of successive alternations of four units of CoO_6 octahedra with a CoO_6 prism.

There are a number of other Sr–Co–O phases reported in literature. However, they were not observed under our sample preparation conditions in this study. For example, Gourdon *et al.*[30] reported modulated structures of the $Sr_{14}Co_{11}O_{33}$ and $Sr_{24}Co_{19}O_{57}$ phases by single crystal growth using the KOH flux in an alumina crucible at 1100 °C. These phases crystallized in incommensurate structures. We did not observe these two phases.

D. SrO–CaO–CoO_x

No ternary oxide phase was found in the SrO–CaO–CoO_x system other than the three solid solution series as a result of the substitution of Ca into the Sr–Co–O compounds or Sr into the Ca sites of the Ca–Co–O compounds. The solid solution, $(Ca,Sr)_3Co_4O_9$, features a misfit layered oxide that has an incommensurate structure.[12] Sr substitutes in the Ca site of $Ca_3Co_4O_9$ to the limit of $(Ca_{0.8}Sr_{0.2})_3Co_4O_9$. The second phase, $(Ca,Sr)_3Co_2O_6$, is the

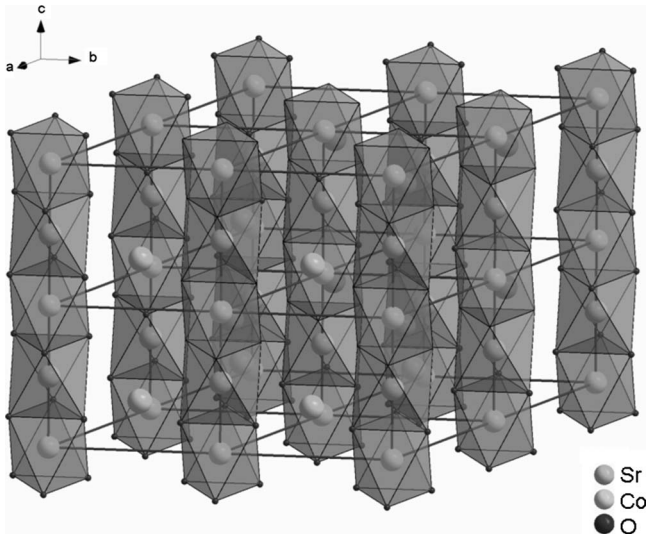

FIG. 8. Crystal structure of $BaCoO_3$ (n=∝ member in the homologous series, $Ba_{n+2}Co_nCoO_{3n+3}$)

n=1 member of the homologous series $(Ca,Sr)_{n+2}Co_nCo'O_{3n+3}$, where Sr substitutes in the Ca site to the limit of $(Ca_{0.9}Sr_{0.1})_3Co_2O_6$. In the third series, $(Sr,Ca)_{n+2}Co_nCo'O_{3n+3}$, Ca substitutes in the Sr site of the n=2, 3, and 4 members to the limit of $(Sr_{0.7}Ca_{0.3})_4Co_3O_9$, $(Sr_{0.67}Ca_{0.33})_5Co_4O_{11}$, and $(Sr_{0.725}Ca_{0.275})_6Co_5O_{13.5}$, respectively. The detailed structure of the phases $(Sr_{0.8}Ca_{0.2})_5Co_4O_{12}$ and $Sr_6Co_5O_{15}$ and their reference x-ray powder diffraction patterns will be reported elsewhere.[31]

In Fig. 1, because of the presence of various solid solutions in the Sr–Ca–Co–O system, series of tie-line bundles are constructed. The $(Ca,Sr)_3Co_2O_6$ phase is compatible with (Ca, Sr)O, $Ca_3Co_4O_9$, and with $(Sr_{0.7}Ca_{0.3})_4Co_3O_9$. The $(Ca,Sr)_3Co_4O_9$ phase is in equilibrium with $(Sr_{0.7}Ca_{0.3})_4Co_3O_9$, $(Sr_{2/3}Ca_{1/3})_5Co_4O_{12}$, $(Sr_{0.725}Ca_{0.275})_6Co_5O_{15}$, and CoO_x. The $Sr_{n+2}Co_nCo'O_{3n+3}$ series is in equilibrium with (Sr, Ca)O and CoO_x.

E. TE properties

TE properties of a number of compounds in the Sr–Co–O and Ca–Co–O systems have been reported in literature.[22,32–38] In the Ca–Co–O system, the $Ca_3Co_4O_9$ phase was reported to exhibit strong anisotropic properties and has good TE property along the *ab* plane. It has very low resistivity. *ZT* was reported to be >1 at 1000 K. It is thought that the increased scattering of phonons at the interface of misfit layers leads to the lowering of the lattice thermal conductivity. The Seebeck coefficient for single crystal $Ca_3Co_2O_6$ has been reported by Mikami and Funahashi[10] to be relatively high and positive, and the thermal conductivity is relatively low at high temperature. The transport properties are dominated mainly by p-type carriers. *ZT* was determined to be about 0.15 at 1000 K for a single crystal of $Ca_3Co_2O_6$. The authors further reported that since the power factor of the n=2 polycrystalline phase, $Sr_4Co_3O_{12}$, has a substantially lower thermal conductivity and higher power factor than the other members of the homogolous series, it is likely that the *ZT* value of the single crystal of $Sr_4Co_3O_{12}$ will be higher than that of $Ca_3Co_2O_6$.

The Seebeck coefficient, thermal conductivity, and resistivity data of selected n=2, 3 and n=4 members of the $(Sr,Ca)_{n+2}Co_nCo'O_{3n+3}$ series, namely, $[(Sr_{0.7}Ca_{0.3})_4Co_3O_9$, $(Sr_{0.8}Ca_{0.2})_5Co_4O_{12}$, and $(Sr_{0.87}Ca_{0.13})_6Co_5O_{15}]$ as a function of temperature are given in Figs. 9(a)–9(c), respectively. In general, the thermal conductivity of all three compounds appears to be low. The resistivity values indicate an activated dependence with temperature, similar to out-of-plane carrier transport observed in $Ca_3Co_4O_9$ (Ref. 12) but with larger magnitudes in part due to the high porosity. Below 200 K the magnitudes are too large for the apparatus to acquire a measurement. The positive Seebeck coefficients suggest hole dominated conduction, with room temperature magnitudes between 110 and 140 μV/K [Fig. 9(a)]. The Seebeck coefficients rise acutely with decreasing temperature with maximum near 200 K, and then decrease rapidly toward zero. We attribute this decrease to the measurement apparatus and not to the intrinsic material properties. The gain settings and instrument impedance, coupled to the large resistivities below

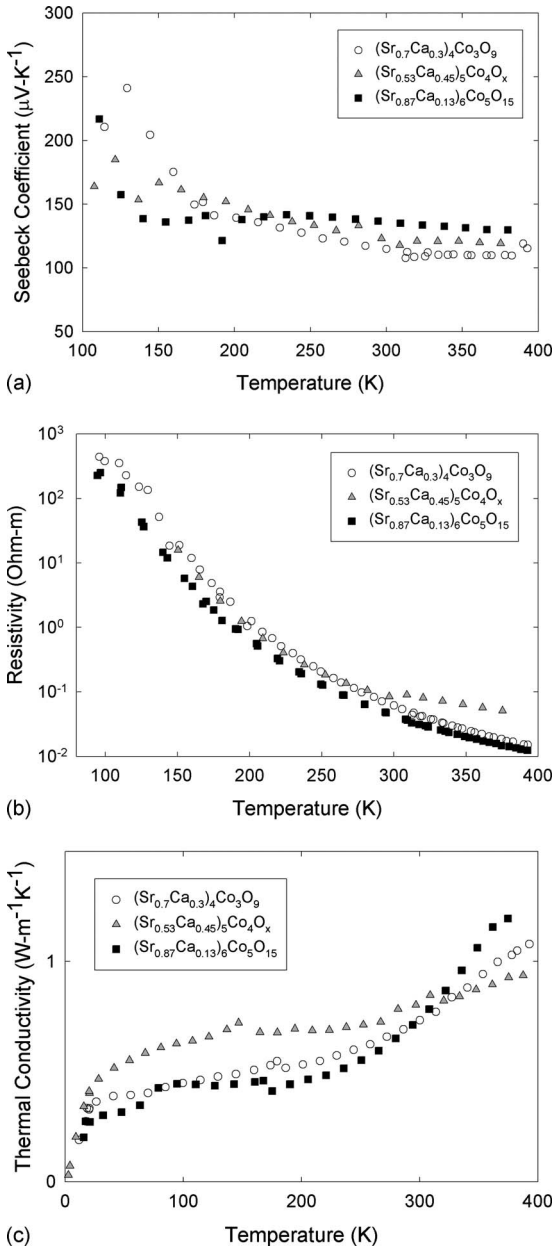

FIG. 9. (a) Seebeck coefficient, (b) resistivity, and (c) thermal conductivity for the n=2 $((Sr_{0.7}Ca_{0.3})_4Co_3O_9)$, n=3 $((Sr,Ca)_5Co_4\ O_{13})$, and n=4 $((Sr_{0.87}Ca_{0.13})_6Co_5O_{15})$ members of $(Sr,Ca)_{n+2}Co_nCoO_{3n+3}$.

200 K, can result in the insulating effects between the voltage probes; thus, small offset currents in the voltmeter adversely impact the data required for proper fitting of the ac voltage/temperature pulse. The magnitudes and temperature dependencies of the transport properties are similar in all three compounds. Although the $(Ca,Sr)_{n+2}Co_nCo'O_{3n+3}$ oxides show relatively high Seebeck coefficients and low thermal conductivities in general, their resistivity values, however, are relatively high.

IV. SUMMARY

The Sr–Ca–Co–O system is an important system for TE research because it consists of two low dimension phases, namely, $(Ca,Sr)_3Co_4O_9$ with misfit layered structure and $(Ca,Sr)_{n+2}Co_nCo'O_{3n+3}$ with one-dimensional cobalt oxide

chains that offer interesting TE properties. The phase diagram of the Sr–Ca–Co–O system that was determined at 850 °C in air offers detailed compatibility relationships in the binary as well as the ternary oxide systems which are important for processing and for the understanding of material properties. The homogeneity range of the $(Ca,Sr)_3Co_4O_9$ and $(Ca,Sr)_{n+2}Co_nCo'O_{3n+3}$ solid solutions has been determined. Although the $(Ca,Sr)_{n+2}Co_nCo'O_{3n+3}$ oxides show relatively high Seebeck coefficient and low thermal conductivity in general, their resistivity values, however, are relatively high. Therefore unless we can decrease the resisitivity via either substitution or improved processing, the best cobaltite material for TE applications, at present, is $Ca_3Co_4O_9$ that features misfit layered structure.

[1]G. S. Nolas, J. Sharp, and H. J. Goldsmid, *Thermoelectric: Basic Principles and New Materials Developments* (Springer, New York, 2001).
[2]T. M. Tritt and M. A. Subramanian, MRS Bull. **31**, 188 (2006).
[3]T. M. Tritt, Science **272**, 1276 (1996).
[4]K. F. Hsu, S. Loo, F. Guo, W. Chen, J. S. Dyck, C. Uher, T. Hogan, E. K. Polychroniadis, and M. G. Kanatzidis, Science **303**, 818 (2004).
[5]R. Venkatasubramanian, E. Siivola, T. Colpitts, and B. O'Quinn, Nature (London) **413**, 597 (2001).
[6]S. Ghamaty and N. B. Eisner, Proceeding of the Eighteenth International Conference on Thermoelectrics, Baltimore, MD, pp. 485-488 (1999).
[7]M. S. Dresselhaus, G. Chen, M. Y. Tang, R. G. Yang, H. Lee, D. Z. Wang, Z. F. Ren, J. P. Fleurial, and P. Gogna, Mater. Res. Soc. Symp. Proc. **886**, 3 (2006).
[8]I. Terasaki, Y. Sasago, and K. Uchinokura, Phys. Rev. B **56**, R12685 (1997).
[9]M. Mikami, R. Funashashi, M. Yoshimura, Y. Mori, and T. Sasaki, J. Appl. Phys. **94**, 6579 (2003).
[10]M. Mikami and R. Funahashi, J. Solid State Chem. **178**, 1670 (2005).
[11]D. Grebille, S. Lambert, F. Bouree, and V. Petricek, J. Appl. Crystallogr. **37**, 823 (2004).
[12]A. C. Masset, C. Michel, A. Maignan, M. Hervieu, O. Toulemonde, F. Studer, and B. Raveau, Phys. Rev. B **62**, 166 (2000).
[13]H. Minami, K. Itaka, H. Kawaji, Q. J. Wang, H. Koinuma, and M. Lippmaa, Appl. Surf. Sci. **197–198**, 442 (2002).
[14]Y. F. Hu, W. D. Si, E. Sutter, and Q. Li, Appl. Phys. Lett. **86**, 082103 (2005).
[15]Powder Diffraction File (PDF), International Centre for Diffraction Data (ICDD), Newtown Square, PA.
[16]A. C. Larson and R. B. von Dreele, GSAS, General Structure Analysis System, U.S. Government Contract No. W-7405-ENG-36 by the Los Alamos National laboratory, which is operated by the University of California for the U.S. Department of Energy, 1992.
[17]Certain trade names and company products are mentioned in the text or identified in illustrations in order to adequately specify the experimental procedures and equipment used. In no case does such identification imply recommendation or endorsement by the National Institute of Standards and Technology.
[18]M. Otani, N. D. Lowhorn, P. K. Schenck, W. Wong-Ng, and M. Green, Appl. Phys. Lett. **91**, 132102 (2007).
[19]M. Otani, K. Itaka, W. Wong-Ng, P. K. Schenck, and H. Koinuma, Appl. Surf. Sci. **254**, 765 (2007).
[20]Physical Proeprty Measurement system (PPMS), manufactured by Quantum Design, San Diego, CA.
[21]W. Wong-Ng, Y. F. Hu, M. D. Vaudin, B. He, M. Otani, N. D. Lowhorn, and Q. Li, J. Appl. Phys. **102**, 33520 (2007).
[22]R. S. Roth, *Proceedings of the User Aspects of Phase Equilibria*, Joint Research Centre, Petten, The Netherlands (Institute of Metals, London, 1990).
[23]T. Takami, H. Ikuta, and U. Mizutani, Jpn. J. Appl. Phys., Part 1 **43**, 8208 (2004).
[24]H. Fjellvåg, E. Gulbrandsen, S. Aasland, A. Olsem, and B. C. Hauback, J. Solid State Chem. **124**, 190 (1996).
[25]K. Boulahya, M. Parras, and J. M. González-Calbet, J. Solid State Chem. **142**, 419 (1999).
[26]K. Boulahya, M. Parras, and J. M. González-Calbet, J. Solid State Chem. **145**, 116 (1999).
[27]M. Huvê, C. Renard, F. Abraham, G. van Tendeloo, and S. Amelinckx, J. Solid State Chem. **135**, 1 (1998).
[28]W. T. A. Harrison, S. I. Hegwood, and A. J. Jacobson, Chem. Commun. (Cambridge) **1995**, 1953.
[29]R. D. Shannon, Acta Crystallogr., Sect. A: Cryst. Phys., Diffr., Theor. Gen. Crystallogr. **32**, 751 (1976).
[30]O. Gourdon, V. Petricek, M. Dusek, P. Bezdicka, S. Durovic, D. Gyepesova, and M. Evain, Acta Crystallogr., Sect. B: Struct. Sci. **55**, 841 (1999).
[31]W. Wong-Ng, G. Liu, and J. A. Kaduk, "Hexagonal Perovskite Related $A_{n+2}B'O_{3n+3}$ (A=Ba, Sr, and Ca) Homologous Series: Crystal Structure and Reference Patterns," Solid State Sci. (submitted).
[32]M. Mikami and R. Funahashi, IEEE Proceedings on 22nd International Conference on Thermoelectrics, pp. 200–202, 2003.
[33]S. Hébert, D. Flahaut, C. Martin, S. Lemonnier, J. Noudem, C. Goupil, A. Maifnan, and J. Hejtmanek, Prog. Solid State Chem. **35**, 457 (2007).
[34]K. Iwasaki, H. Yamane, S. Kubota, J. Takahashi, and M. Shimada, J. Alloys Compd. **358**, 210 (2003).
[35]Y. Miyazaki, Solid State Ionics **172**, 463 (2004).
[36]S. Li, R. Funahashi, I. Matsubara, H. Yamada, K. Ueno, and S. Sodeoka, Ceram. Int. **27**, 321 (2001).
[37]S. Li, R. Funahashi, I. Matsubara, H. Yamada, K. Ueno, S. Sodeoka, and H. Yamada, Chem. Mater. **12**, 2424 (2000).
[38]M. Prevel, O. Perez, and J. G. Noudem, Solid State Sci. **9**, 231 (2007).